14th European Signal Processing Conference (EUSIPCO 2006), Florence, Italy, September 4-8, 2006, copyright by EURASIP

A NOVEL FOCUSING TECHNIQUE FOR ISAR IN CASE OF UNIFORM ROTATION RATE

J.M. Muñoz-Ferreras and F. Pérez-Martínez

Department of Señales, Sistemas y Radiocomunicaciones, Universidad Politécnica de Madrid
Avda. Complutense s/n, 28040, Madrid, Spain
phone: + (34) 913367358, fax: + (34) 913367362, email: jmmunoz@gmr.ssr.upm.es
web: www.gmr.ssr.upm.es

ABSTRACT

A method for the correction of Migration Through Resolution Cells (MTRC) in ISAR (Inverse Synthetic Aperture Radar) is addressed here. The new technique needs neither to know the target motion parameters, to estimate them nor to use optimization to maximize (minimize) an image focusing indicator. It assumes that the target rotation rate is uniform and the direction of the effective rotation vector does not change during the Coherent Processing Interval (CPI). The algorithm corrects the MTRC in two phases: Slant Range Rotation Compensation (SRRC) and Cross Range Rotation Compensation (CRRC), where CRRC is based on an extension of the Phase Difference method (PD). The effectiveness of the proposed technique is verified with simulated (MIG-25 aircraft) and real (sailboat) radar data and compared with the standard Range-Doppler Algorithm (RDA).

1. INTRODUCTION

ISAR is a radar technique to obtain high resolution images of non-cooperative targets [1]. These images can be used to recognize and identify targets (Automatic Target Recognition, ATR) in all-weather conditions, overcoming the limitations of the optical systems. The coherent nature of the technique allows to obtain characteristic target signatures, such as micro-Doppler information [2], which can help in the recognition/identification task.

The ISAR images are usually contaminated with blurring artifacts due to the target motion. In general, the target motion can be divided in translational and rotational components, whose blurring effects must be corrected.

The translational motion compensation works in two steps: range alignment and phase compensation. Range alignment methods are envelope correlation [1], global range alignment [3] and so on. Important phase compensation algorithms are dominant scatterer algorithm [4], phase gradient autofocus [5], AUTOCLEAN method [6], minimum entropy method [7] and contrast maximization technique [8]. Here the translational motion compensation is assumed to be done.

However, the target rotation can also cause blurring effects on the ISAR image: the MTRC [9]. The MTRC is evident with the increase of the resolution in the systems [9]. The Polar Formatting Algorithm (PFA), [10], can correct the MTRC, but it needs an accurate estimate of the target rotational motion, which is not always possible. Ref. [11] and [12] propose methods to estimate the rotation parameters, but they suppose the existence of dominant scatterers, which moreover could have migrated in slant range. An optimization method is proposed in [13], which is computationally costly and can suffer with multi-modal functions. The AJTF (Adaptive Joint Time-Frequency) technique opened the area of time-frequency transforms to compensate target motion [14]. Recently, keystone formatting has been used to correct MTRC [15].

In this paper a method for MTRC correction is addressed. It does make use neither of the estimation of the motion parameters nor of optimization. The method is an extension of [16] and [17]. In this paper a modification of PD for the CRRC phase is proposed, instead of entropy minimization methods. Simulated (MIG-25 aircraft) and real (sailboat) radar data are used to verify the technique.

2. EXISTENCE OF MTRC

It exists MTRC when the target scatterers migrate in slant range or cross range cells during the CPI. J. L. Walker [9] gives the conditions that must meet the target dimensions to guarantee that there is no MTRC

$$D_{\mathrm{r}} \leq \frac{4 \cdot \rho_{\mathrm{a}}^2}{\lambda} \tag{1}$$

$$D_{\mathrm{a}} \leq \frac{4 \cdot \rho_{\mathrm{a}} \cdot \rho_{\mathrm{r}}}{\lambda}, \tag{2}$$

where D_{r} and D_{a} are the target dimensions in slant and cross range, respectively, ρ_{r} and ρ_{a} are the range and cross range resolutions, respectively, and λ is the transmitted wavelength.

The slant and cross range resolutions, ρ_{r} and ρ_{a}, are given by

$$\rho_{\mathrm{r}} = \frac{c}{2 \cdot B} \tag{3}$$

$$\rho_{\mathrm{a}} = \frac{\lambda}{2 \cdot \theta_{\mathrm{t}}}, \tag{4}$$

where c is the light speed, B is the transmitted bandwidth and θ_{t} is the total aspect angle change of the target during the CPI.

Supposing, for example, an aspect angle change of 5° during the CPI, a transmitted bandwidth of 1 GHz and a wavelength of 0.01 m, which are similar to the parameters when capturing the real data shown in this paper, the slant and cross range resolutions are 0.15 m and 0.06 m, respectively. This means that the maximum target dimensions to guarantee that there is no MTRC are 1.3 m in slant range and 3.4 m in cross range.

Many real targets (sailboats, for example) have greater dimensions and can suffer from MTRC. An increase in the

transmitted bandwidth, in which we are working, would make worse the situation. Therefore, an MTRC compensation algorithm is necessary.

3. MTRC CORRECTION

After translational motion compensation, the target can be seen as a rotating object. A scatterer on the target migrates in range and cross range during the CPI. If the variation in the target aspect angle is small, it can be shown that the migration in slant range of the scatterer in slow time τ is

$$\Delta Y(\tau) = X \cdot \Delta\theta(\tau), \tag{5}$$

where $\Delta Y(\tau)$ is the migration in slant range, X is the original position (with respect to the rotation center) of the scatterer ($\tau = 0$) in cross range and $\Delta\theta(\tau)$ is the change in the aspect angle.

In cross range the rotational motion generates a space-variant phase error [17], which can be approximated by

$$\varphi_e(\tau) = -\frac{2\cdot\pi}{\lambda} \cdot \left[Y \cdot (\Delta\theta(\tau))^2\right], \tag{6}$$

where Y is the original position (with respect to the rotation center) of the scatterer ($\tau = 0$) in slant range.

3.1 Slant Range Rotation Compensation (SRRC)

Assuming that the rotation rate is uniform during the CPI, the cross range position X can be expressed as

$$X = i \cdot \rho_a = i \cdot \frac{\lambda}{2 \cdot M \cdot \delta\theta}, \tag{7}$$

where i is the number of the cross range cell X, M is the total number of cross range cells and $\delta\theta$ is the aspect angle change between two pulses.

On the other hand, the aspect angle change $\Delta\theta(\tau)$ can be expressed as

$$\Delta\theta(\tau) = j \cdot \delta\theta, \tag{8}$$

where j is the number of pulse (number of observation).

Combining (7) and (8) in (5), the migration in slant range is independent of $\delta\theta$, as shown by (9).

$$\Delta Y(\tau) = i \cdot j \cdot \frac{\lambda}{2 \cdot M}. \tag{9}$$

Assuming that the rotation rate is uniform during the CPI and taking into account (9), we can correct the migration due to the rotation component in slant range without a priori knowledge nor the estimation of the target motion parameters and without the use of computationally costly optimization techniques. For each cross range cell i, the SRRC algorithm shifts each pulse according to (9).

3.2 Cross Range Rotation Compensation (CRRC)

This process is posterior to the SRRC algorithm. If we assume a uniform rotation rate, the phase error given in (6) can be expressed as follows

$$\varphi_e(\tau) = -\frac{2\cdot\pi}{\lambda} \cdot \left[Y \cdot \Omega^2 \cdot \tau^2\right], \tag{10}$$

where Ω is the uniform rotation rate.

Ref. [16] proposes an entropy minimization technique to remove this error, which can be computationally costly and can suffer from the possible existence of local minima. Ref. [17] supposes that the rotation rate is known, what is not true in scenarios with non-cooperative targets.

Equation (10) is a quadratic phase error (QPE) in slow time τ, which is space-variant in slant range. This error can be corrected with MapDrift and PD [10]. Nevertheless, we choose PD since it is more efficient than MapDrift. Since the QPE is space-variant, it is not possible to estimate one phase error for all the range cells, as it is proposed in [10] in the context of SAR (Synthetic Aperture Radar).

In the CRRC technique we propose, a quadratic coefficient is estimated for each range cell. PD is run independently for each phase history (for each range cell). If all the quadratic coefficients were well estimated, we would obtain a linear profile when representing the estimated quadratic coefficient vs. the number of slant range cell, according to (10). Moreover, the range cell with the lowest absolute value of the estimated quadratic coefficient corresponds to the slant range position of the rotation center.

Nevertheless, PD can misestimate the quadratic coefficient in some of the range cells. This is a well known result and its cause is that the peak position of the Fourier transform of the product of the first subaperture by the complex conjugate of the second subaperture does not always indicate the value $a \cdot T_a$, where a is the quadratic coefficient to be estimated and T_a corresponds to the CPI. The correct indication of $a \cdot T_a$ depends strongly on the spectral content of each slow-time history (each range cell).

The effect of the previous problem is that the profile of the quadratic coefficient vs. the number of slant range cell has outliers, which abandon the linear tendency indicated in (10). Fig. 1a presents this profile for the MIG-25 data. We can see a linear tendency with the existence of outliers.

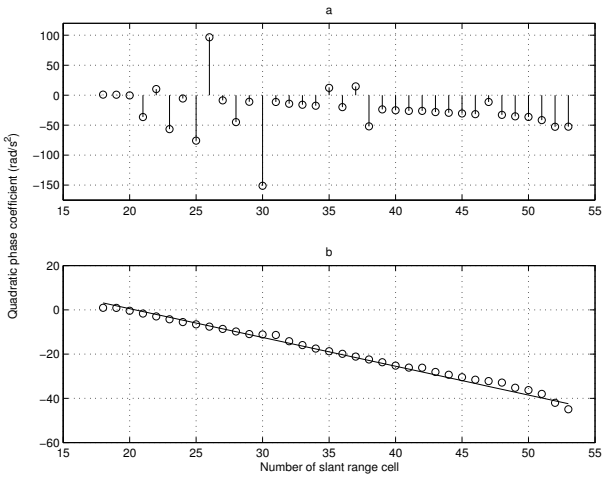

Figure 1: (a) Quadratic coefficient vs. slant range cell profile (MIG-25) (b) Outliers deletion and linear regression (MIG-25)

Fortunately, not all the quadratic coefficients are estimated incorrectly. Generally, it is possible to identify the expected linear tendency in the profile. This identification allows to assign the correct quadratic coefficients to the corrupted slant range bins.

In this work, the adequate assignment of the quadratic coefficients is made manually. The circles (○) in Fig. 1b show the result of the manual process for the MIG-25 data, while the line indicates a linear regression of the ○ values. These are the values used to compensate the space-variant QPE. In the future, automatic statistical methods for this estimation will be investigated. As a note, we can infer that the rotation center corresponds to the range cell 20, since it has the lowest absolute value of the estimated quadratic coefficient.

Once the correct estimations of the quadratic coefficients have been obtained, the CRRC algorithm modifies the phase of each slant range cell, multiplying each phase history (each range cell) by the conjugate of the exponential term shown in (11).

$$s_{\mathrm{c}}(\tau) = e^{j\cdot\hat{a}\cdot\tau^2}. \tag{11}$$

Therefore, a complete MTRC compensation is possible without the need of knowledge nor estimation of the rotation motion parameters. Optimization techniques are not necessary either. The proposed technique assumes that the rotation rate is uniform during the CPI and that the effective rotation vector does not change its direction during the CPI.

4. RESULTS

In this section results of the proposed technique with simulated and real data are shown. Table 1 presents the radar parameters for the simulated MIG-25 data. The simulated aircraft is composed of 120 point scatterers of equal reflectivity.

Table 1: Radar Parameters for Simulation

Radar type	Stepped frequency
Central frequency (f_0)	9 GHz
Wavelength (λ)	0.033 m
Stepped frequencies in a burst	64
Number of bursts	512
Pulse Repetition Frequency (PRF)	15000 Hz
Bandwidth (B)	512 MHz
Range Resolution (ρ_{r})	0.3 m

Fig. 2 shows the ISAR image constructed using simple FFTs (Fast Fourier Transform), what is the base of RDA. The blurring effects due to the MTRC are evident. Fig. 3 presents the ISAR image after SRRC, where the slant range migration has been corrected and Fig. 4 shows the final output after CRRC. A focused ISAR image of the MIG-25 aircraft is obtained. The representation of these figures is in decibels, so that (12) is used

$$\mathbf{I}|_{\mathrm{dB}} = 20\cdot\log\mathbf{I}, \tag{12}$$

where $\mathbf{I}$ is the absolute value of the ISAR image normalized by its maximum and $\mathbf{I}|_{\mathrm{dB}}$ is the normalized ISAR image in decibels.

Our research group has developed an LFMCW (Linear Frequency Modulated Continuous Wave) millimeter-wave radar prototype [18]. Its parameters are detailed in Table 2. Fig. 5a shows the ISAR image of a sailboat produced without using any focusing algorithm. Fig. 5b, Fig. 5c and Fig. 5d

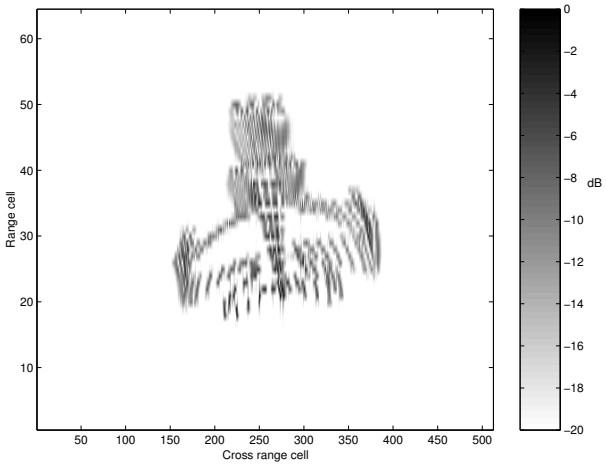

Figure 2: ISAR image of MIG-25 data using basic RDA (Existence of MTRC)

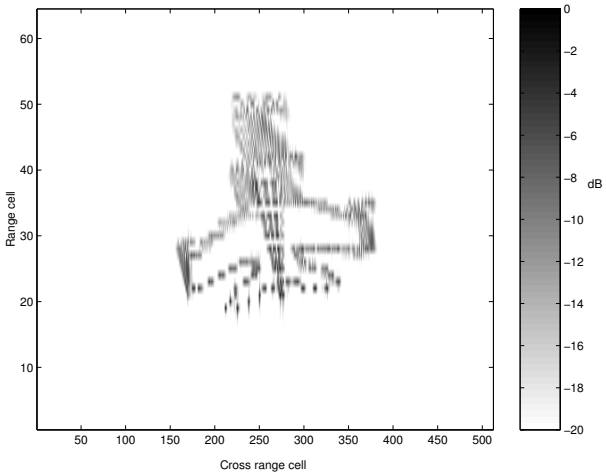

Figure 3: ISAR image of MIG-25 data after SRRC (Correction of slant range migration)

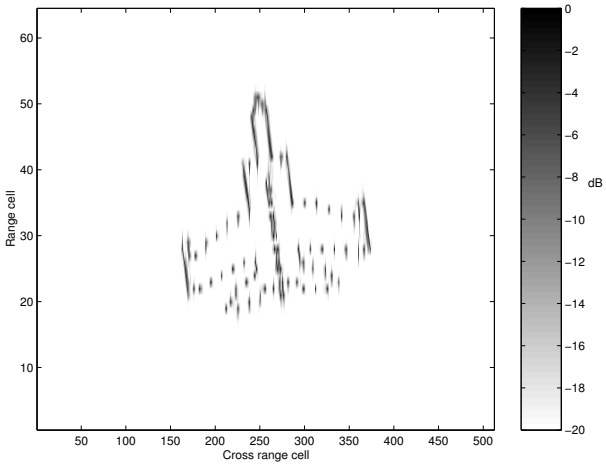

Figure 4: ISAR image of MIG-25 data after CRRC (Correction of cross range migration)

show the ISAR images after basic translational motion compensation, after SRRC and after CRRC, respectively. The increase in focus in each phase is evident. A highly zoomed photo of the sailboat at the moment of the capture of the data is shown in Fig. 5e. In order to obtain the final ISAR image, neither knowledge nor estimation of the target rotation parameters have been necessary.

Table 2: Real Radar Parameters

Radar type	LFMCW
Central frequency (f_0)	28.5 GHz
Wavelength (λ)	0.0105 m
Pulse Repetition Frequency (PRF)	1000 Hz
Transmitted Bandwidth (B)	1 GHz
Processed Range Resolution (ρ_r)	0.2 m

5. CONCLUSIONS

A new method for the MTRC correction in ISAR images has been presented. The novel technique needs neither to know nor to estimate the target rotation parameters. It does not use optimization-based methods either. The effectiveness of the approach has been verified with both simulated and real data from a non-cooperative target.

ACKNOWLEDGMENTS

This work was supported by the Projects TIC02-04569-C02-01 and TIC02-02657-C02-01 of the National Board of Scientific and Technology Research. The authors thank Dr. V.C. Chen for providing the simulation data of the MIG-25 aircraft.

REFERENCES

[1] C. C. Chen and H. C. Andrews, "Target Motion Induced Radar Imaging," *IEEE Transactions on Aerospace and Electronic Systems*, Vol. 16, No. 1, pp. 2–14, 1980.

[2] V. C. Chen, F. Li, S.-S. Ho and H. Wechsler, "Analysis of micro-Doppler signatures," *IEE Proceedings on Radar, Sonar and Navigation*, Vol. 150, No. 4, pp. 271–276, August 2003.

[3] J. Wang and D. Kasilingam, "Global Range Alignment for ISAR," *IEEE Transactions on Aerospace and Electronic Systems*, Vol. 39, No. 1, pp. 351–357, January 2003.

[4] B. D. Steinberg, "Microwave Imaging of Aircraft," *Proceedings of the IEEE*, Vol. 76, No. 12, pp. 1578–1592, 1988.

[5] D. E. Wahl, P. H. Eichel, D. C. Ghiglia and C. V., Jr., Jakowatz, "Phase gradient autofocus - A robust tool for high resolution SAR phase correction," *IEEE Transactions on Aerospace and Electronic Systems*, Vol. 30, No. 3, pp. 827–835, July 1994.

[6] J. Li, R. Wu and V. C. Chen, "Robust Autofocus Algorithm for ISAR Imaging of Moving Targets," *IEEE Transactions on Aerospace and Electronic Systems*, Vol. 37, No. 3, pp. 1056–1069, July 2001.

[7] L. Xi, L. Guosui and J. Ni, "Autofocusing of ISAR Images Based on Entropy Minimization," *IEEE Transactions on Aerospace and Electronic Systems*, Vol. 35, No. 4, pp. 1240–1252, October 1999.

[8] F. Berizzi and G. Corsini, "Autofocusing of Inverse Synthetic Aperture Radar Images using contrast maximization," *IEEE Transactions on Aerospace and Electronic Systems*, Vol. 32, No. 3, pp. 1185–1191, July 1996.

[9] J. L. Walker, "Range-Doppler Imaging of Rotating Objects," *IEEE Transactions on Aerospace and Electronic Systems*, AES-16, pp. 23–52, 1980.

[10] W. G. Carrara, R. S. Goodman and R. M. Majewski, *Spotlight synthetic aperture radar: Signal processing algorithms*. Artech House, Boston-London, 1995.

[11] R. Lipps and D. Kerr, "Polar Reformatting for ISAR imaging," *1998 National Radar Conference*, Dallas, 12–13 May 1998.

[12] S. Werness, W. Carrara, L. Joyce and D. Franczak, "Moving Target Imaging Algorithm for SAR Data," *IEEE Transactions on Aerospace and Electronic Systems*, Vol. 26, No. 1, January 1990.

[13] B. C. Flores and A. Ugarte, "An approach to angular motion compensation in ISAR imagery," *Antennas and Propagation Society International Symposium*, 1992. AP-S. 1992 Digest. 18-25 July 1992, pp. 1106–1109, Vol. 2.

[14] Y. Wang, H. Ling and V. C. Chen, "ISAR Motion Compensation Via Adaptive Joint Time-Frequency Technique," *IEEE Transactions on Aerospace and Electronic Systems*, Vol. 34, No. 2, pp. 670–676, April 1998.

[15] M. Xing, R. Wu, J. Lan and Z. Bao, "Migration Through Resolution Cell Compensation in ISAR Imaging," *IEEE Geoscience and Remote Sensing Letters*, Vol. 1, April 2004.

[16] G. Y. Lu and Z. Bao, "Compensation of scatterer migration through resolution cell in inverse synthetic aperture radar imaging," *IEE Proceedings on Radar, Sonar and Navigation*, Vol. 147, No. 2, April 2000.

[17] A. Aprile, A. Mauri and D. Pastina, "Real time rotational motion compensation algorithm for focusing spot-SAR/ISAR images in case of variable rotation-rate," *First European Radar Conference, 2004, EURAD 2004*, 11-15 October 2004, pp. 141–144.

[18] A. Blanco-del-Campo, A. Asensio-López, B. P. Dorta-Naranjo, J. Gismero-Menoyo, D. Ramírez-Morán, C. Carmona-Duarte and J. L. Jiménez-Martín, "Millimeter-wave radar demonstrator for high resolution imaging," *First European Radar Conference, 2004, EURAD 2004*, 11-15 October 2004, pp. 65–68.

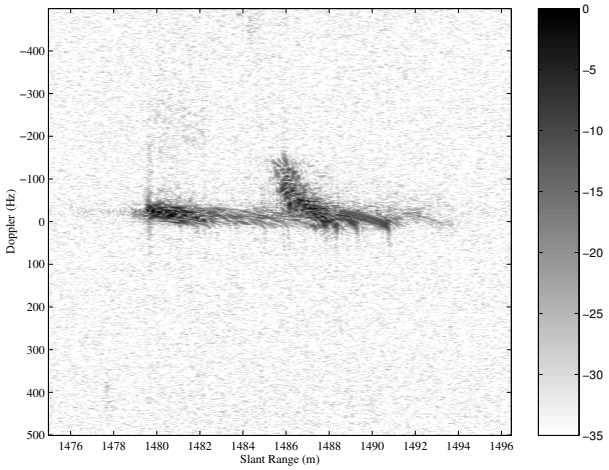

(a) Using RDA (without translational nor rotational motion compensation)

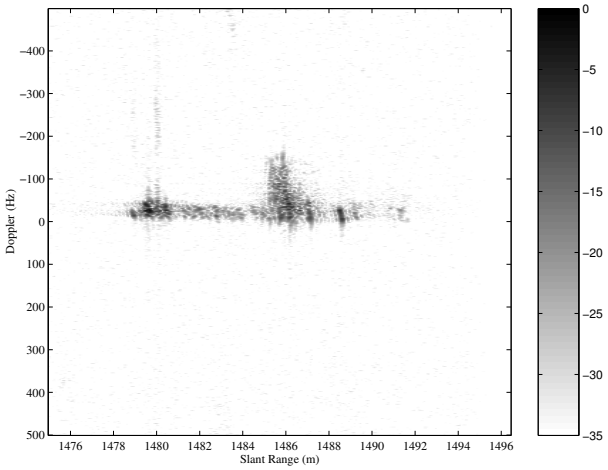

(b) After translational motion compensation

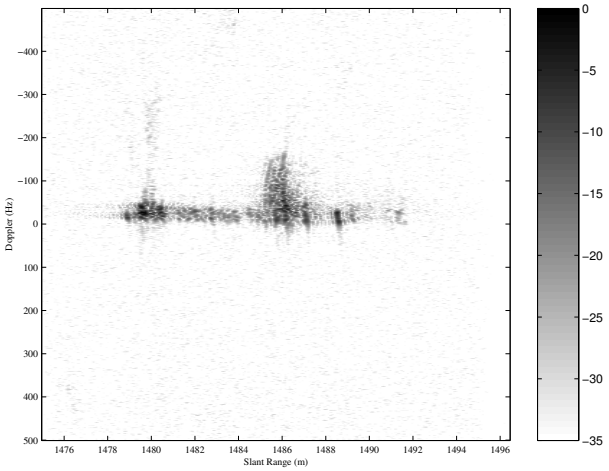

(c) After SRRC (Correction of slant range migration)

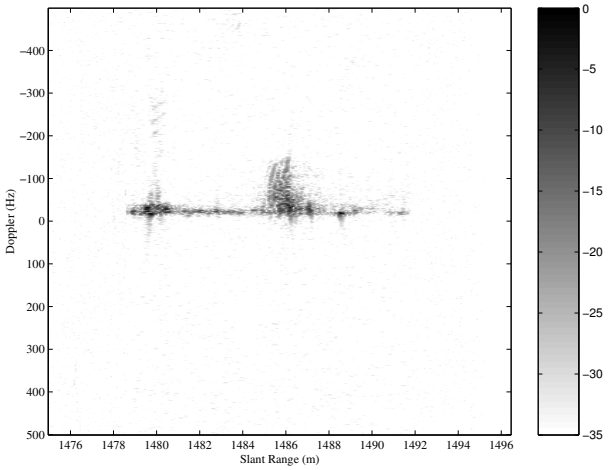

(d) After CRRC (Correction of cross range migration)

(e) Highly zoomed photo of the sailboat at the moment of capturing the data

Figure 5: ISAR images and photo of a sailboat